Intermediate-Spin State of a 3d Ion in the Octahedral Environment and Generalization of the TanabeÀSugano Diagrams

DATASET · APRIL 2013

CITATION
1

READS
31

8 AUTHORS, INCLUDING:

Karina Lamonova
National Academy of Sciences of Ukraine
31 PUBLICATIONS **224** CITATIONS
SEE PROFILE

E. S. Zhitlukhina
13 PUBLICATIONS **76** CITATIONS
SEE PROFILE

THE JOURNAL OF PHYSICAL CHEMISTRY A

ARTICLE

pubs.acs.org/JPCA

Intermediate-Spin State of a 3d Ion in the Octahedral Environment and Generalization of the Tanabe−Sugano Diagrams

Karina V. Lamonova,*[,†] Elena S. Zhitlukhina,[†] Roman Yu. Babkin,[†] Sergei M. Orel,[†] Sergei G. Ovchinnikov,[‡] and Yurii G. Pashkevich[†]

[†]O. O. Galkin Donetsk Institute for Physics and Engineering, National Academy of Sciences of Ukraine, 83114 Donetsk, Ukraine

[‡]L. V. Kirensky Institute of Physics, Siberian Branch of the Russian Academy of Sciences, 660036 Krasnoyarsk, Russia

ABSTRACT: Electronic spectra of $3d^n$ transition ions in an octahedral ligand surrounding have been studied using the modified crystal field approach (MCFA), which includes a relativistic spin−orbital interaction. A new variable parameter, the effective nuclear charge Z_{eff} of a metal ion that allows accounting implicitly the covalence degree of a metal−ligand bond, has been introduced. Energy diagrams similar to the Tanabe−Sugano ones have been calculated. To study the spin state evolution of the metal ion in an arbitrary distorted octahedral complex, a spin state diagram approach has been proposed. The intermediate-spin (IS) state problem for $3d^4$, $3d^5$, and $3d^6$ metal ions has been considered and conditions for the IS state realization have been formulated. The regions of the mixed high-, intermediate-, and low-spin states have been found. The possibility of coexistence of the different spin states of 3d ions in the octahedral complexes has been considered using crystallography data for the $YBaCo_2O_{5.5}$ layered cobaltite.

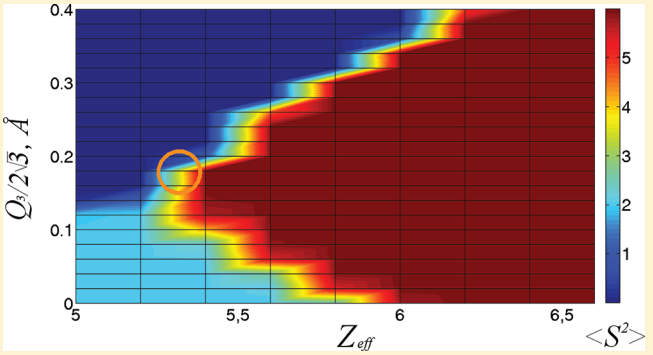

1. INTRODUCTION

It is well-known that the terms of the ions with $3d^4$, $3d^5$, and $3d^6$ electronic configurations can be classified into three spin states: the high-spin (HS) state ($S = 2$ for $3d^4$ and $3d^6$ ions and $S = 5/2$ for $3d^5$ ones), the low-spin (LS) state ($S = 0$ for $3d^4$ and $3d^6$ ions and $S = 1/2$ for $3d^5$ ones), and the state with intermediate spin (IS) ($S = 1$ for $3d^4$ and $3d^6$ ions and $S = 3/2$ for $3d^5$ ones). The existence of an intermediate-spin state in the ions placed in the octahedral complexes is a long-standing problem of *physical chemistry*, in particular, *quantum chemistry*. The IS state never is the ground state in the ligand-field theory. However, currently there is a large number of experimental data confirming that the intermediate-spin state can be realized in octahedral complexes, which are building blocks of different functional mediums. For instance, spin state stability in the cobalt-containing oxides[1−6] is one of the most debated issues in recent years. This question is relevant for one of the most rapidly developing and promising scientific areas that can be called molecular nanomagnetism.[7] It includes various iron based spin crossover systems, discovered in the 1930s by Cambi in organic ferromagnets,[8−10] and also low-dimensional magnets like single molecule magnets and single chain magnets.[2,11,12]

Traditionally, the problem of the ground state of 3d ions in coordination complexes is solved by the crystal field theory (CFT) that is the most simple but quite effective semiempirical method.[13,14] Restriction of the CFT to the electrostatic nature of interaction between d ion and ligands reduces strongly its application because the electron structure of ligand ions is not considered. Nevertheless, the CFT enables us to perform analysis of the electronic state splitting and symmetry, to predict the transitions between electronic states. It can be used to predict chemical properties, kinetic properties, reaction mechanisms, magnetic and spectral properties, and thermodynamic data. Moreover, the CFT allows tracing the evolution of relative energies and spin states at the changing complex symmetry without using cumbersome ab initio computational methods. Obviously, semiempirical and ab initio procedures for the electronic spectra problem are not mutually exclusive and the most rational way to further studies lies in their combination and in finding a "golden mean".

In this paper we have investigated the electronic spectra of the transition ions with $3d^n$ ($n = 2−8$) electronic configurations, which are placed in the undistorted and arbitrary distorted $[ML_6]$ octahedral complexes with the modified crystal field approach (MCFA).[15,16]

The basic MCFA statements are as follows:

(a) The Born−Oppenheimer approximation is inherently assumed; however, wave functions are the functions of ligand nuclear coordinates as the variable parameters.

(b) The basis set of the eigenfunctions corresponding to the specific $3d^n$ configuration includes the finite number of orthogonal antisymmetric many-electron wave functions,

Received: July 26, 2011
Revised: September 20, 2011
Published: September 21, 2011

which are composed of the hydrogen-like functions with effective nuclear charge Z_{eff} as the variable parameter.

(c) The spin−orbit interaction is taken into account.

We have calculated the energy levels (energy diagrams) for $3d^n$ ($n = 2-8$) electronic configurations without accounting for spin−orbital interactions and plotted ones like the Tanabe−Sugano diagrams. However, unlike traditional Tanabe−Sugano diagrams we used the effective nuclear charge Z_{eff} instead of the crystal field splitting Δ_{CF} as the variable parameter. The value Δ_{CF} is experimentally measurable, and it depends on several parameters of coordination complex: the ligand charges, the effective nuclear charge, and the set of ligand coordinates. If one varies Δ_{CF}, it is impossible to determine the cause of the energy spectrum rearrangement, because each of above-mentioned parameters has different effects on the crystal field splitting. The traditional CFT does not allow exploring the other types of distortion beyond the breathing-mode distortion. On the contrary, the MCFA allows calculation with arbitrary symmetry of coordination complexes and arbitrary sets of ligand charges that significantly expands the applications of the method. The changing of Z_{eff} allows us to account implicitly the covalence degree of "metal−ligand" bond.

By the MCFA technique we have calculated the spin state diagrams $\langle S^2\rangle = f(Z_{eff}, Q_i)$, which account for the spin−orbital interaction and can be plotted in the parametric space "effective nuclear charge - arbitrary distortions of $[ML_6]$ complex" at the fixed ligand charge value. Using the spin state diagrams, the spin state of 3d ion can be predicted and the reason for spin state transformations can be established. In this paper we have obtained conditions for the implementation of the intermediate-spin state in the octahedral complexes. Namely, we have found the range of variation of the effective nuclear charge Z_{eff} for a given distortion of $[ML_6]$ complex and the range of distortion changing.

2. THEORETICAL BASIC: THE MODIFIED CRYSTAL FIELD APPROACH

Let us consider the regular octahedral complex $[ML_6]$ with a metal ion with $3d^n$ electronic configuration ($1 < n < 9$). The ligand ions are located in the octahedral vertexes and the metallic ion is in the center of the octahedron.

In the framework of MCFA the calculation of wave functions of the metal ion complex requires the solution of the Schrödinger equation with a full many-electron Hamiltonian:

$$H = H_0 + V \tag{1}$$

where H_0 is the kinetic energy of the electrons and the atom nuclear; $V = V_{EE} + V_{CF} + V_{SO} + V_H$ is the operator sum of the electron−electron correlation between 3d electrons, the interaction of the d-shell electrons with a ligand crystal field, the spin−orbit interaction, and the interaction with an external magnetic field, respectively. So, the perturbation operator is written as

$$V = \sum_{i>j}^{n} \frac{e^2}{r_{ij}} + \sum_{k=1}^{N}\sum_{i=1}^{n} \frac{eq_k}{|\vec{r}_i - \vec{R}_k|} + \sum_{i=1}^{n} \xi(r_i)(\vec{l}_i, \vec{s}_i) + \mu_B \sum_{i=1}^{n} (\vec{l}_i + 2\vec{s}_i, \vec{H}) \tag{2}$$

Here n is the number of valence electrons in the central ion, N is the number of ligand ions, q_k is the charge fixed at $\vec{R}_k$, H is the external magnetic field, μ_B is Bohr's magneton, $\vec{l}_i$ and $\vec{s}_i$ are the operators of orbital and spin moments for the ith electron, and $\xi(r_i)$ is an single-electron constant of a spin−orbit interaction. The SO interaction has traditional form:

$$a(r_i) = -\frac{e\hbar^2}{2m^2c^2}\frac{1}{r_i}\frac{\partial U(r_i)}{\partial r_i} \tag{3}$$

where $U(r_i)$ is a field potential for an electron.

The SO coupling constant, characterizes the splitting of atomic levels associated with the spin−orbit interaction:

$$\xi_{n_i l_i} = \int a(r) R_{n_i l_i}{}^2(r) r^2 \, dr \tag{4}$$

where $R_{n_i l_i}$ represents the electron radial functions with the principal n and orbital l quantum numbers.

To calculate $\xi_{n_i l_i}$, it is necessary to find the explicit form of a spherical symmetric potential $U(r)$, which is quite a complicated task. As a rule, one approximates the form of potential by a simple semiempirical formula [more detail see in ref 17]

$$\xi_{nl} = \frac{\alpha^2}{2}\frac{Z^{\delta-\beta}\overline{Z}_{eff}^{4-\delta}}{n_*{}^3 l(l+1)(l+1/2)} \qquad (\delta = 0, ..., 4) \tag{5}$$

where $\alpha = e^2/\hbar c$ is the fine structure constant, n_* is the effective principal quantum number,[18] and $\overline{Z}_{eff}$ is the improved value of the effective nuclear charge.[17] The parameter δ is fitting one so that the calculated spin−orbital splitting coincides with the value of $\xi_{n_i l_i}$ measured experimentally for a free ion. The spin−orbital splitting constant with $\delta = 2$ most accurately describes the electronic spectrum of corresponding free ion. Moreover, we have introduced into the formula (5) the amendment $Z^{-\beta}$, which allows us to adjust the value of the single-electron constant $\xi_{n_i l_i}$ with respect to the experimental one, as well as to correct the positions of the spectral energy levels of the metal ion. Choice of the form of the spin−orbital constant can also implicitly take into account other relativistic effects, despite the fact that they are not involved when the spectrum is calculated.

To calculate the eigenvalues of the perturbation operator (2), we use the full orthonormalized system of the many-electron symmetry-adapted functions $\Psi(\gamma SLM_S M_L)$, which correspond to the $3d^n$ configuration. The functions $\Psi(\gamma SLM_S M_L)$ are the term wave functions given by the linear combinations of the *many-electron determinant functions* $\Phi(1, 2, ..., n)$ (the numbers correspond to the number of single-electron wave functions $\psi_i(nlm_l m_s)$ for each of the 3d valence electrons[14]). For the single-electron wave functions we take the hydrogen-like wave functions with an effective parameter $a = Z_{eff}/n_* a_0$ (a_0 the Bohr's radius). In such case, the matrix elements have a form

$$V_{\alpha\beta} = \langle \Psi_\alpha(\gamma SLM_S M_L)|V|\Psi_\beta(\gamma' S' M_S' M_L')\rangle \tag{6}$$

To conclude this section, we should note that the effective nuclear charge is an independent variable and in the simplest case of octahedral symmetry[14,19] the parameters Δ_{CF} and Z_{eff} are interconnected as follows:

$$\Delta_{CF} = \frac{5}{3} eq \cdot F_4(R) \tag{7}$$

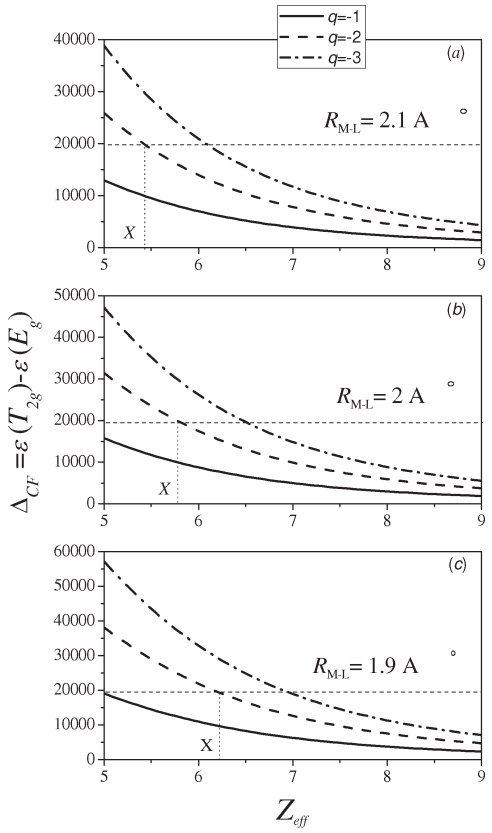

Figure 1. Crystal field splitting Δ_{CF} vs Z_{eff} at given parameters: (a) R_{M-L} = 2.1 Å; (b) R_{M-L} = 2 Å; (c) R_{M-L} = 1.9 Å.

where

$$F_4(R) = \frac{1}{R^5}\int_0^R r^6 R_{3d}{}^2(r)\,dr + R^4\int_R^\infty r^{-3} R_{3d}{}^2(r)\,dr$$

$$R_{3d}(r) = \frac{4}{3\sqrt{10}}\,a^{7/2} r^2 \exp(-ar) \qquad a = Z_{eff}/na_0$$

The dependence $\Delta_{CF} = \Delta_{CF}(Z_{eff})$ is shown in Figure 1. The crystal field splitting decreases when the effective nuclear charge magnitude tends to the free metal ion one. The increase of the ligand charge leads to the increase of the $\Delta_{CF} = \varepsilon(T_{2g}) - \varepsilon(E_g)$ splitting. In turn, the bond length increase results in the crystal field decrease. The same magnitude of the splitting corresponds to the different values of bond lengths and effective nuclear charges (see, for instance, displacement of a point *X* in Figure 1a−c).

3. COMPARISON OF CLASSICAL TANABE−SUGANO DIAGRAMS WITH THE $E = E(Z_{EFF})$ ENERGY DIAGRAMS OBTAINED BY THE MCFA

In this section we present calculations of the electronic energy levels of the transition metal with $3d^n$ electronic configurations located in the basal plane of a regular octahedral complex $[ML_6]$. The parameters of the problem are the effective nuclear charge Z_{eff}, the set of ligand charges q_k, and the set of ligand coordinates $\{R_k\}$. As concerns a ligand in all cases, we consider the divalent oxygen ion O^{2-}. Hence, $q_1 = ... = q_6 = -2$ and the bond length between 3d metal and oxygen ions is $R_{M-O^{2-}} = 2$ Å. The metal−oxygen bond length selected for calculating the energy diagrams is the average because the sum of ionic radii of oxygen and metal ions varies from 1.88 Å for Mn^{4+} to 2.25 Å for Cr^{+}. (Ionic radius, calculated by Shannon[20] for the free ion O^{2-} in the VI-order coordination equals $R(O^{2-}) \approx 1.35$ Å.) The surrounding crystal field has different effect on various metal ions. For some of them there are slightly compressed oxygen core, usually it happens for ions M^{2+} (M = Ti, V, Cr, Mn, Co, Ni). The trivalent M^{3+} (M = V, Cr, Mn, Fe, Co, Ni) and tetravalent ions M^{4+} (M = Cr, Mn, Fe) can be considered as almost free.

In the beginning we have examined the problem when the spin−orbit coupling is ignored. In this case the electron−electron interaction between d-electrons and its interaction with surrounding crystal field (first and second terms in (2)) determine the ground spin state. A competition between these interactions leads to the different spin state transitions. The electron−electron repulsion seeks to establish a high-spin state in the 3d ion in accordance with the Hund's rule. At the same time the interaction between d-electrons and the surrounding crystal strives against Hund's order and leads to the spin reduction. We have constructed the energy diagrams $\Delta E = \Delta E(Z_{eff})|_{R=2Å}$ like theTanabe−Sugano diagrams (Figure 2).

For instance, the calculations show that the ions with $3d^2$, $3d^3$, and $3d^8$ electronic configurations do not reveal any spin state transformations in all ranges over Z_{eff} (see Figure 2a,b,g). The ground high-spin level lies very low, and the energy distance from it to the nearest excited level is very large. It means that only very destructive octahedral distortions can lead to spin state transformations. Notice beforehand that the homogeneous compressing of octahedral complex, in other words the decrease of bond length ($R_{M^{x+}-O^{2-}}$) in reasonable limits does not result in the spin state transformations in these cases. The picture becomes more complicated for $3d^{4-7}$ configurations (Figure 2c−f). The lowest levels correspond to the high-spin state. However, action of the octahedral crystal field results in the changing of the ground spin state of the metal ion at the *A*, *B*, *C*, and *D* points, which are the random degeneration points. Similar transformations can be initiated by thermal distortions of the crystal structure, by applying hydrostatic pressure or magnetic/electric fields.

Bearing in mind that the implementation of a free ion in the crystal medium leads to a decrease of the effective nuclear charge of 10−15% for divalent and 15−20% for trivalent ions,[21] one can determine the range of Z_{eff} that corresponds to the ion state in particular environment. In other words, one approximately can determine the starting state point. There are some schemes for calculating the Z_{eff},[18,22−26] and the final result depends on the choice of a particular scheme. For instance, the effective nuclear charges of Cr^{2+} and Mn^{3+} ions with $3d^4$ electronic configuration calculated according to the Slater scheme[18] are equal to 4.95 and 5.95, respectively. These values correspond to the intermediate- (S = 1) and the high-spin (S = 2) states (Figure 2c). By placing the ions in the regular six-coordinate complex $[MO_6]$ with the bond length $R_{M-O^{2-}}$ = 2 Å, one can expect that in the first case the value of Z_{eff} will decrease by 10−15%, i.e., become equal to Z_{eff} = 4.21, and in the second case by 20%, i.e., Z_{eff} = 4.76. Thus, the spin state of chromium ion Cr^{2+} does not change, whereas the spin state on manganese Mn^{3+} becomes S = 1 (Figure 2c). If the effective nuclear charges take values calculated in ref 17, Z_{eff} = 6.22 for Cr^{2+} and Z_{eff} = 7.55 for Mn^{3+}, then both ions are in the high-spin states. In the crystal field Z_{eff} values reduced to 6.04 and 5.29; i.e., Cr^{2+} and

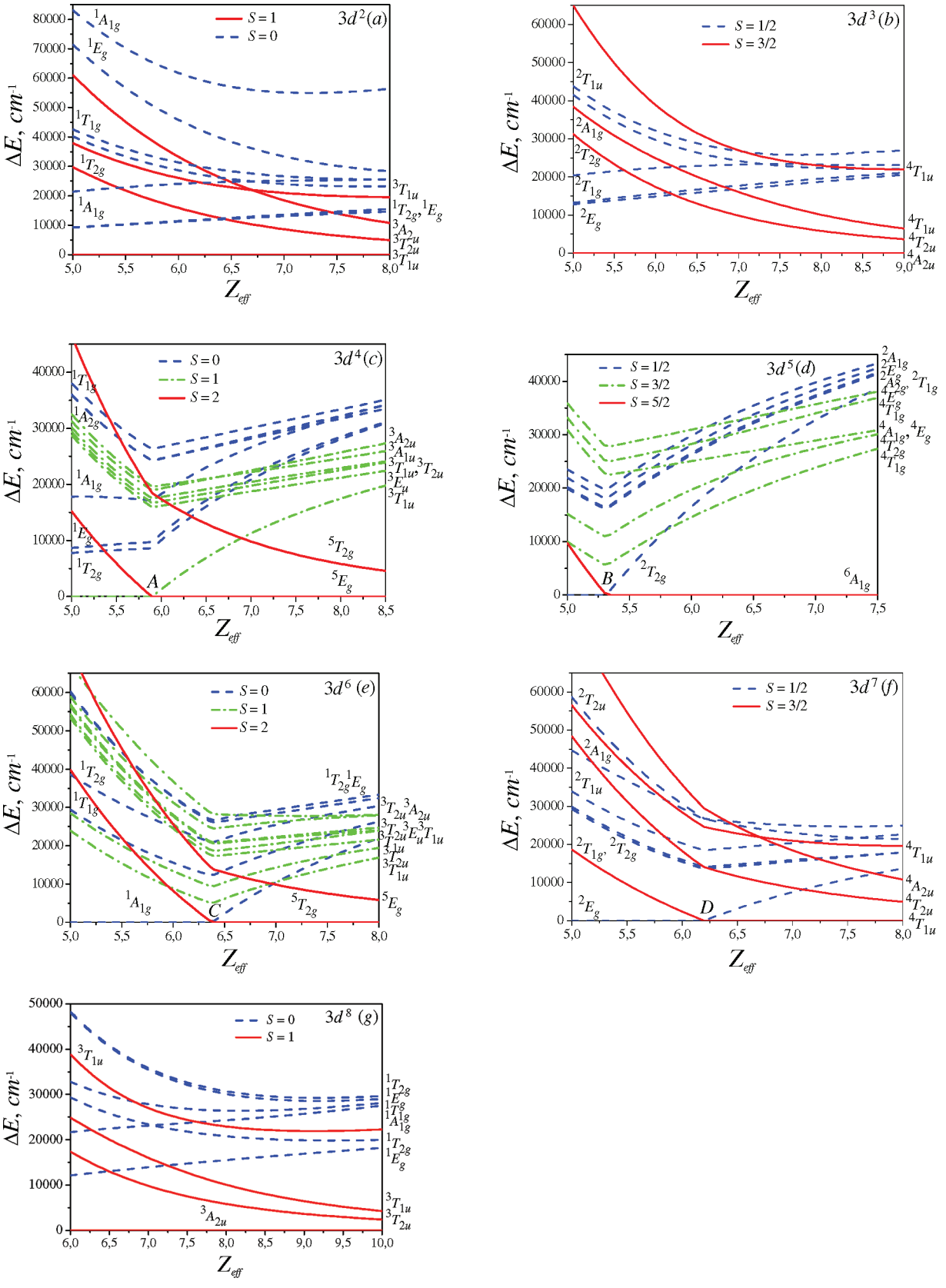

Figure 2. Energetic diagrams $\Delta E = \Delta E(Z_{\text{eff}})|_{R=2\text{Å}}$ like theTanabe−Sugano ones for $3d^n$ electronic configuration ($n = 2-8$).

Mn^{3+} ions are in the states with $S = 1$ and $S = 2$, respectively. This contradiction shows that to identify the ion spin state the value of Z_{eff} should be known more accurately or found from the experimental data. The MCFA allows determining the value

dx.doi.org/10.1021/jp2071265 |J. Phys. Chem. A 2011, 115, 13596–13604

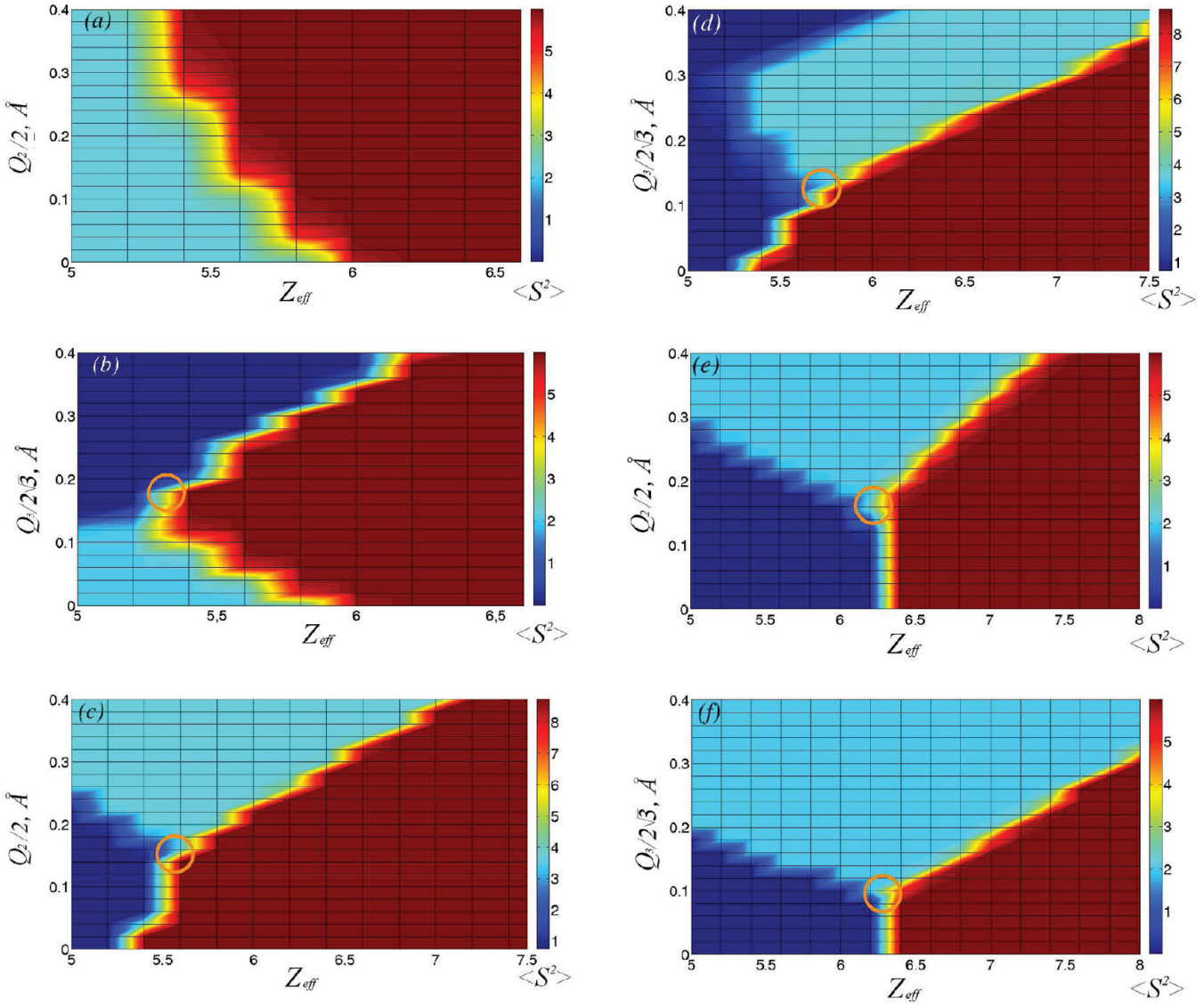

Figure 3. Spin state diagrams $\langle S^2 \rangle = f(Z_{eff}, Q_{(2,3)})$ for the metal ions with $3d^{4-6}$ electronic configuration: $3d^4$ (a) and (b); $3d^5$ (c) and (d); $3d^6$ (e) and (f).

of the effective nuclear charge from the experimental values of the *g*-factor.[27,28]

In conclusion, one should note that in the absence of distortion our energy diagrams reproduce the Tanabe−Sugano diagrams. The value of the effective nuclear charge depends on the crystal field modification in a general case. The homogeneous deformation of the coordination complex and its deformation with symmetry reduction results into the redistribution of electron density in the space of metal-oxide complex and to the Z_{eff} decrease.

4. EFFECT OF THE OCTAHEDRAL COMPLEX DISTORTIONS ON THE $3D^N$ ION SPECTRA: SPIN STATE DIAGRAMS $\langle S^2 \rangle = F(Z_{EFF}, Q_I)$

We emphasize that the method of the MCF has the capability to calculate the electronic energy levels of an arbitrary distorted coordination complex with the spin−orbit interaction of the transition metal. In this section we will consider the spin state diagrams that account for the spin−orbital interaction. The spin state diagram $\langle S^2 \rangle = f(Z_{eff}, Q_i)$ presents the average spin square as a function of effective nuclear charge (Z_{eff}) and arbitrary distortions of [ML_6] complex (Q_i) at the fixed ligand charge values. Here one should note that the effective nuclear charge and the ligand charges both result in a change of the crystal field. However, the change of Z_{eff} as follows from (7) has a more substantial influence on the crystal field value than a change of the ligand charges q_k.

Spin state diagrams in Figure 3 demonstrate the transformation of the spin state of the transition metal ion on the plane of two parameters, the effective nuclear charge Z_{eff} and different octahedral distortions described by the normal coordinates Q_i corresponding to the O_h point symmetry group.[19] The dependence of the single-electron spin−orbit constant on Z_{eff} allows us implicitly to take into account the effects that are beyond the approximation of the ionic bond and obtain accurate quantitative results.

dx.doi.org/10.1021/jp2071265 |*J. Phys. Chem. A* 2011, 115, 13596–13604

We have considered some kinds of normal distortions that are the most typical for the octahedral coordination in the real compounds. They are the E_g distortions ($Q_2 = (x_2 - x_5 - y_3 + y_6)/2$, $Q_3 = (2z_1 - 2z_4 - x_2 + x_5 - y_3 + y_6)/2$) or tetragonal Jahn−Teller ones (subsection 4.1) and also T_{2g} distortions ($Q_4 = (z_3 - z_6 + y_1 - y_4)/2$, $Q_5 = (x_1 - x_4 + z_2 - z_5)/2$, $Q_6 = (y_2 - y_5 + x_3 - x_6)/2$) or trigonal ones (subsection 4.2). The same calculations have been performed in ref 19 for the pyramidal complex with the $3d^4(3d^6)$ metals.

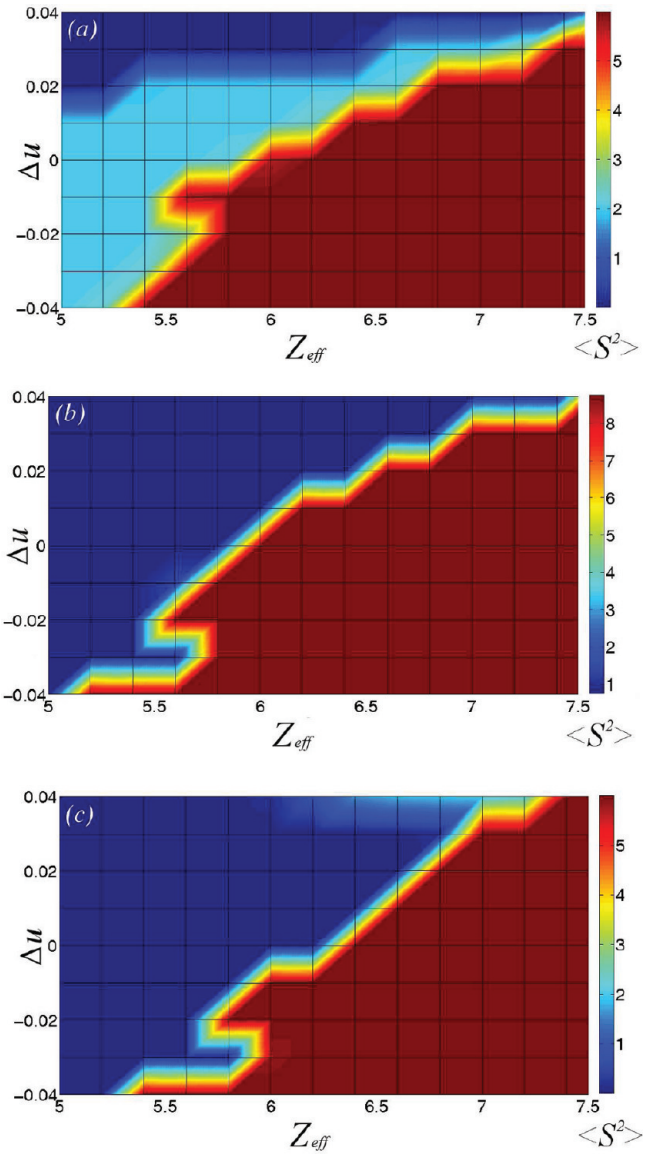

Figure 4. Spin state diagrams $\langle S^2 \rangle = f(Z_{eff}, \Delta u)$: (a) $3d^4$; (b) $3d^5$; (c) $3d^6$.

4.1. Tetragonal Jahn−Teller Distortions (Q_2, Q_3). The calculations of the spin state diagrams for the $3d^2$, $3d^3$, $3d^8$, and $3d^7$ ions have revealed that the HS ↔ LS spin state transformations require rather large Jahn−Teller distortions. It is a predictable result, because the lowest energy level with a HS state is far from the nearest excited level with a LS state (Figure 2a,b,f,g).

The situation is of interest for other electronic configurations. Spin state diagrams for the metal ions with $3d^{4-6}$ electronic configuration constructed on the plane of variables "effective nuclear charge, e_g distortions" demonstrate very nontrivial behavior of the spin subsystem of metal ions (Figure 3). One can see some colored regions corresponding to the different spin states of a metal ion: the red region for the high-spin state, the green region for the intermediate-spin state, and the blue one for the low-spin state. Moreover, there are three boundary areas related to the mixed spin states. They are HS:LS, IS:LS, and HS:LS mixed spin boundary areas, which are realized in accordance with the type of the electronic configuration. The existence of such mixed regions results from the spin−orbit interaction. Due to this coupling the quantum operators $\hat{S}_z$ and $\hat{S}^2$ are not conserved ones; i.e., they are "bad quantum numbers". In spite of this fact, the values of $\hat{S}_z$ and $\hat{S}^2$ characterize the degree of mixing of different spin states.

It is interesting to note that the mixed spin areas are quite narrow in the case of an octahedron surrounding in comparison with a pyramidal one,[16] and one can consider it as transition "lines". Figure 3 shows that these lines have the different forms in the dependence on the distortion type.

Moreover, there are areas that could be called "the triple points". In their vicinities the eigenfunctions corresponding to the three different spin states are mixed (they are marked in Figure 3b−f the yellow solid circles). It means that in these areas the spin subsystem is very unstable and is sensitive to the insignificant atom displacements. Note that the position of the triple point is not fixed and varies depending on the type of distortion and on the electronic configuration. In the spin state diagrams like $\langle S^2 \rangle = f(Z_{eff}, Q_3)$ one can see that with increasing number of electrons the "triple point" is shifted to higher Z_{eff} values and lower Q_3 distortion ones. This means that ions with

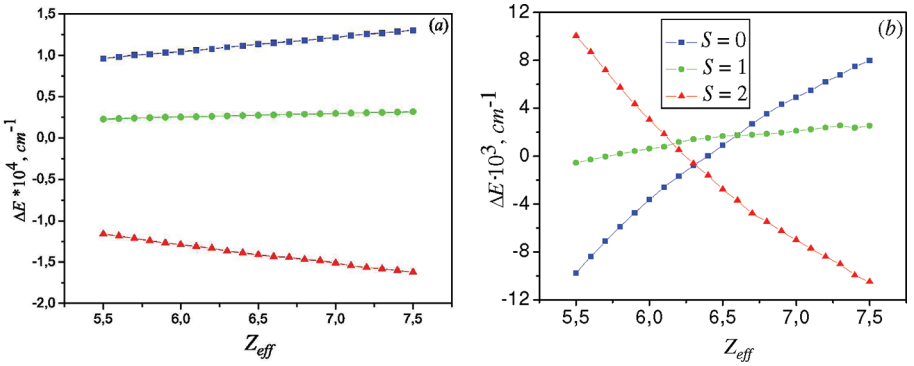

Figure 5. Energy diagrams for the Co^{3+} ions in the octahedral environments at the $T = 293$ K: (a) for the Co(1) position; (b) for the Co(2) position.

dx.doi.org/10.1021/jp2071265 |J. Phys. Chem. A 2011, 115, 13596–13604

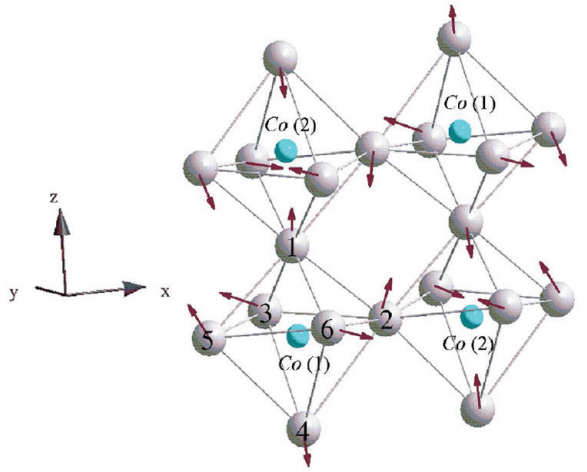

Figure 6. Fragment of the $YBaCo_2O_{5.5}$ crystal structure with real distortions.

$3d^6$ configurations are more sensitive to crystal field changes than the $3d^4$ ions.

Using the spin state diagrams, one can formulate the conditions for the realization of the IS state in the presence of Jahn−Teller distortions. Figure 3 shows that in the absence of distortions the Z_{eff} reduction results in the HS ↔ LS transitions except for $3d^4$ ions for which it is the HS ↔ IS one. The onset of the Jahn−Teller distortion (for instance, see Figure 3b) leads to a cascade of spin state transitions like IS ↔ HS ↔ LS before "the triple point" or IS ↔ LS after it.

4.2. Trigonal Distortions (Q_4, Q_5, Q_6). The trigonal distortions (Q_4, Q_5, Q_6) are often encountered in real compounds, for example, in compounds with the spinel structure AB_2O_4. They are transformed by the irreducible representation T_{2g} of an O_h group. The atomic coordinates of conventional spinel structure are as follows: A^{2+} 8a(1/8, 1/8, 1/8), B^{3+} 16d(1/2, 1/2, 1/2), and O^{2-} 32e(u, u, u). If $u = u_0 = 0.25$, the spinel structure is ideal, and the site symmetry of the B ion corresponds to the group O_h. If $u \neq u_0$, the site symmetry of the B ion reduces to D_{3d}, and there are trigonal distortions of the octahedral complexes $\{BO_6\}$ that can be described by a linear combination of T_{2g} normal coordinates like $Q_{trig} = (Q_4 \pm Q_5 \pm Q_6)/3^{1/2}$. They can be expressed in u-terms: $Q_4 = 2(u - 1/4)$, $Q_5 = Q_6 = -2(u - 1/4)$. The spin state diagrams for $3d^{4-6}$ electronic configurations on the plane of "effective nuclear charge − the trigonal distortion $\Delta u = u - u_0$" are represented in Figure 4.

It is seen that in the case of a $3d^4$ configuration such distortions result in the intermediate-spin state in a wide range of parameters (Z_{eff}, Δu). In the case of the $3d^5$ configuration, the trigonal distortions initiate the HS ↔ LS spin crossover transitions. As for the $3d^6$ configuration, the state with $S = 1$ can be implemented with $Z_{eff} \approx 7$ and $\Delta u \geq 0.04$. Finally, note that there are no "triple points" in the $\langle S^2 \rangle = f(Z_{eff}, \Delta u)$ diagrams.

5. COEXISTENCE OF DIFFERENT SPIN STATES ON THE NEIGHBORING OCTAHEDRONS

The spin state instability in three-dimensional compounds may occur in various manifestations. Some of them proceed as a gradual and random replacement of HS states to LS states under temperature decrease as it takes place in the octahedron corner-shared perovskite $LaCoO_3$.[3,29,30] Another variant is the

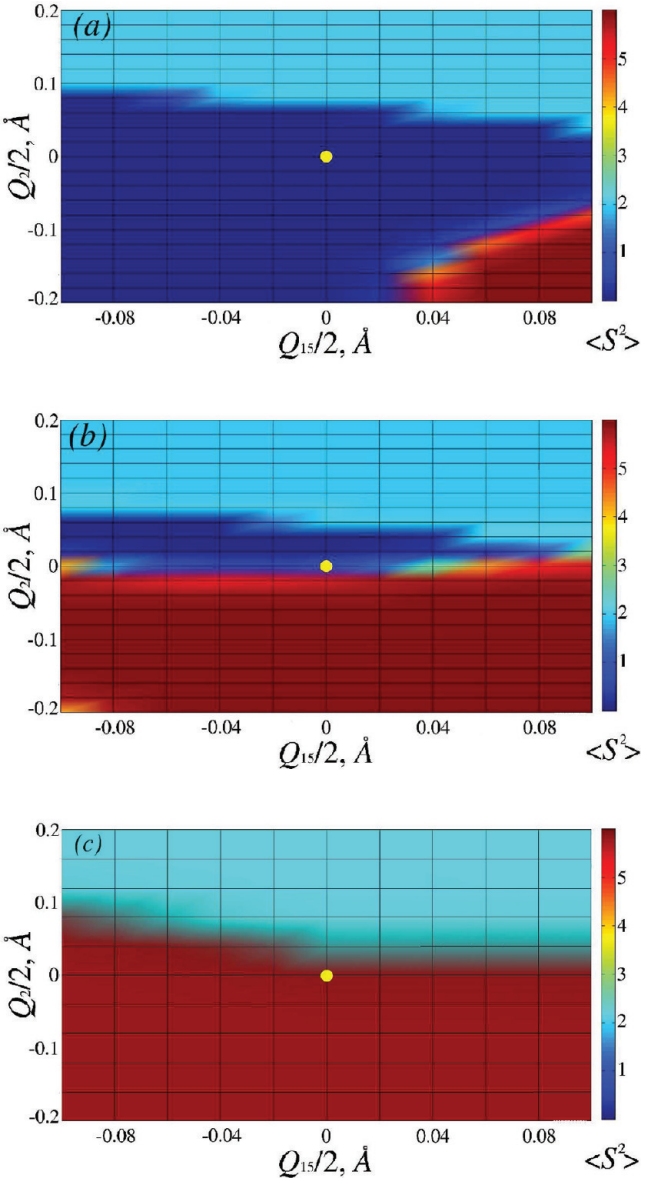

Figure 7. Spin state diagrams for the Co(2) ion at given values of Z_{eff} in the plane of the additional distortions (Q_2, Q_{15}): (a) $Z_{eff} = 6.2$; (b) $Z_{eff} = 6.3$; (c) $Z_{eff} = 6.4$.

no uniform configuration of different spin states on neighboring sites, which can be stable in some temperature regions. Such a situation is realized, for instance, in layered cobaltites.[31] As follows from our analysis and the Tanabe−Sugano diagrams, such a coexistence is possible in the case of corner shared octahedrons. Indeed, to obtain a HS−LS checkerboard-like distribution, it is necessary to have simultaneous stretching/compression distortions of neighboring octahedrons. Such a situation has been modeled in ref 32. Much more difficult to realize is the coexistence of HS and IS states because there are restrictions to the size of the unit cell and the symmetry of distortions. However, the experimental evidence for HS−IS spin state distribution has been obtained for $RBaCo_2O_{5.5}$ (R = Y, Tb, Dy, Ho) using the muon-spin relaxation technique.[31]

Here we study the conditions for realization of HS and IS spin states of the neighboring octahedral positions, depending on the

Table 1. Distortions in Octahedral Complexes $[Co(1)O_6]^{9+}$ and $[Co(2)O_6]^{9+}$ in the Compound $YBaCo_2O_{5.5}$ at Room Temperature[33] [a]

$[Co(1)O_6]^{9+}$	$[Co(2)O_6]^{9+}$
$Q_{01}(A_{1g}) = -0.072$ Å	$Q_{01}(A_{1g}) = 0.072$ Å
$Q_{02}(E_g) = (x_2 - x_5 - y_3 + y_6)/2 = 0.0495$ Å	$Q_{02}(E_g) = (x_2 - x_5 - y_3 + y_6)/2 = -0.177$ Å
$Q_{03}(E_g) = (2z_1 - 2z_4 - x_2 + x_5 - y_3 + y_6)/2\cdot 3^{1/3} = -0.0753$ Å	$Q_{03}(E_g) = (2z_1 - 2z_4 - x_2 + x_5 - y_3 + y_6)/2\cdot 3^{1/3} = -0.1085$ Å
$Q_{09}(T'_{1u}) = (z_2 + z_5 + z_3 + z_6)/2 = 0.498$ Å	$Q_{09}(T'_{1u}) = (z_2 + z_5 + z_3 + z_6)/2 = -0.55$ Å
$Q_{012}(T''_{1u}) = (z_1 + z_4)/2^{1/2} = 0.0311$ Å	$Q_{012}(T''_{1u}) = (z_1 + z_4)/2^{1/2} = -0.0318$ Å
$Q_{015}(T_{2u}) = (z_2 + z_5 - z_3 - z_6)/2 = 0.182$ Å	$Q_{015}(T_{2u}) = (z_2 + z_5 - z_3 - z_6)/2 = -0.234$ Å

[a] The numeration of the ligand ions is used similar to that of ref 22 and is shown in Figure 6.

distortions of the octahedral crystal field within the MCFA. This analysis is directed to shed light on the *principal* possibility of coexistence of HS−IS spin states on the neighboring octahedral sites and does not pretend on a quantitative answer.

To be more realistic, we consider the structural data for $YBaCo_2O_{5.5}$ compound with the $[CoO_6]^{9-}$ coordination complexes as structural units.[33−36] At given oxygen content all cobalt ions have the oxidation number 3+ and occupy four nonequivalent crystallographic positions in the elementary cell: two of them are in distorted $[CoO_6]^{9-}$-octahedral environments and two others are in distorted $[CoO_5]^{7-}$-pyramidal cages. The lattice structure of $RBaCo_2O_{5.5}$ consists of *ac*-planes of $[CoO_6]^{9-}$ octahedra linked by dual rows of $[CoO_5]^{7-}$ pyramids directed along the *a*-axis. Every two pyramidal chains are separated from each other by the empty channel of oxygen vacancies. Various magnetic structures with different spin state content in the $RBaCo_2O_{5.5}$ have been revealed by the muon spin relaxation measurements.[31] The main conclusion from these studies is that the temperature evolution of the spin state ordering of Co^{3+} ions is mainly connected with the spin state redistribution at octahedral sites whereas the pyramidal sites remain in the intermediate-spin state.

As a first step in our modeling, we calculated the energy levels of a trivalent cobalt ion in the octahedral coordination on the basis of the room temperature crystallographic data[33] for the Z_{eff}. (The effective nuclear charge of free Co^{3+} is equal to 7.25,[18] so this point one may consider as the starting one. In the crystalline environment this value is reduced by 15−20% until 5.8).

Figure 5 demonstrates that within the range of the effective nuclear charge the Co(1) ions are in high-spin state ($S = 2$), whereas the Co(2) ions are in high-spin ($S = 2$) and in low-spin state ($S = 0$). Meanwhile, according to the work[31] at the room temperature the Co(1) ions are in high-spin state and the Co(2) ions are in the intermediate-spin state ($S = 1$). Thus, the energy diagrams constructed on the basis of crystallographic data of ref 33 at the room temperature do not give the desired result, at least for the Co(2) ions.

What are the conditions for implementing the intermediate-spin state for the cobalt ions? To answer this question, we must determine the types of distortions of the coordination complexes $[Co(1)O_6]^{9+}$ and $[Co(2)O_6]^{9+}$ in $YBaCo_2O_{5.5}$ at $T = 293$ *K*, and then by varying the existing distortions in the acceptable range to find which ones are responsible for realization of the intermediate-spin state. Note that the variation of symmetry allowed normal coordinates must be constrained to keep the cell parameters constant. The other restriction comes from the request that coordination complexes $[Co(1)O_6]^{9+}$ and $[Co(2)O_6]^{9+}$ share four common oxygen ions forming a chessboard plane of $[CoO_6]$ octahedra shown in Figure 6.

Our analysis (see the Appendix) has revealed that the distortions of $[Co(1)O_6]^{9+}$ coordination complex are less sizable than the distortions of $[Co(2)O_6]^{9+}$ one. In other words, the octahedral core of the Co(2) ion is more flexible with respect to any distortions; hence the Co(2) ion is more likely to change its spin state under the influence of octahedral distortions.

The model calculations of the energy diagrams like $\Delta E = \Delta E(Q_i)|_{Z_{eff}=const}$ (i = 2, 3, 9, 12, 15 is the number of normal coordinate) have been performed for both octahedral complexes and revealed that only normal distortions like Q_{02} and Q_{015} lead to the rearrangement energy levels of the $[Co(2)O_6]^{9+}$ complex. As for the Co(1) ion, it remains in the high-spin ground state under the influence of the above-mentioned distortions. More elaborate analysis including the spin−orbit interaction is presented in the spin state diagram in Figure 7.

The zero point (yellow circle) on the diagrams corresponds to the spin state of the cobalt ion determined by a given value of the effective nuclear charge and the coordinates of the oxygen ions taken from ref 33 at room temperature. At $Z_{eff} = 6.2$ the basic state of the Co(2) ion is the LS one, at $Z_{eff} = 6.4$ it is the HS one, and at $Z_{eff} = 6.3$ the electronic subsystem of Co(2) ion is in the mixed HS:LS region. The spin state of the Co^{3+} ion is extremely sensitive not only to deformation of the oxygen core but also to a change in the effective nuclear charge. To transfer the system from a state with high or low spin to the state with intermediate spin, it is necessary to make the additional distortions like Q_2, so that Q_2 should be more than 0.2 Å. The point of $Z_{eff} = 6.3$ is the most realistic option for realization of the IS state.

Finally, we arrive at a conclusion about the coexistence of different spin states on neighboring Co^{3+} ions that are placed in the chessboard octahedral plane. As we mentioned above, the distortion of shared oxygen ions at the Co(2) site creates the same distortion with opposite sign at the Co(1) site. If this distortion for instance is the Q_2-type, then (Figure 7c) it has a crucial impact on the change of the Co(2) spin state. At the same time the Co(1) spin state is not sensitive to these distortions. So, it remains in HS states. These results can qualitatively explain the experimental observation of very rich and complex spin state phases that have been detected by the muon spin resonance studies of $RBaCo_2O_{5.5}$.

6. CONCLUSION

We have presented the application of the modified crystal field theory to explain the electronic spectra of 3d ions placed in the octahedral coordination complexes with arbitrary symmetry. The energy diagrams like $\Delta E = \Delta E(Z_{eff})$ at the given coordinates and ligand charges can be calculated in the frame of this method without spin−orbital interaction. For a regular octahedron we

have reproduced the well-known Tanabe−Sugano diagrams. Our approach allows us to include spin−orbital interaction and to generalize the Tanabe−Sugano diagrams by calculation the spin state diagrams. These diagrams describe the evolution of the 3d ion ground spin state in the parameter space "effective nuclear charge − arbitrary distortions of coordination complex". We have found the "triple points" where three different spin states are mixed. With the help of the spin state diagrams we have revealed the conditions for appearance of the intermediate-spin state. Namely, for the $3d^4$ ions the occurrence of both Jahn−Teller and trigonal distortions results in an IS state, whereas for the $3d^5$ and $3d^6$ ions the IS state occurs only in the presence of Jahn−Teller distortions. In the absence of distortions the reducing of Z_{eff} results in the usual HS ↔ LS transitions except for $3d^4$ ions for which it is HS ↔ IS. The magnitude of the Jahn−Teller distortions affects the position of the "triple point" as well as the consequence of the spin state transitions. Our qualitative analysis has demonstrated the possibility of coexistence of IS and HS spin states on the neighboring cobalt ions disposed in the plane of corner shared octahedral $[CoO_6]$ coordination complexes.

APPENDIX

In Table 1 we present the distortions in the octahedral complexes of $[Co(1)O_6]^{9+}$ and $[Co(2)O_6]^{9+}$ in the compound $YBaCo_2O_{5.5}$ at room temperature[33] from a regular octahedron with bond length Co−O R_0 = 1.93 Å.

It should be noted that the $[Co(1)O_6]^{9+}$coordination complex is slightly compressed relative to the regular octahedron (i.e., a high-symmetry distortion like breathing-mode Q_1 equals Q_{01} = −0.072 Å), and the $[Co(2)O_6]^{9+}$ one is a bit stretched (Q_{01} = 0.070 Å). Second, the coordination complexes $[Co(1)O_6]^{9+}$ and $[Co(2)O_6]^{9+}$ are connected by common oxygen ions, as shown in Figure 6. Therefore, the Q_{02}-type distortions have opposite signs; i.e., the octahedral planes undergo a rhombic distortion in the different directions: the $[Co(1)O_6]^{9+}$ complex is distorted in the *x*-axis, and the $[Co(2)O_6]^{9+}$ complex in *y*-axis. The magnitude of the Q_2-type distortions differs by almost 3 times. The Q_{03}-type distortions have the same signs, and their values do not differ so dramatically. Finally, the distortions like Q_{09} (displacement of the ligands that are in the octahedral plane along the *z*-axis), Q_{012} (displacements of apical ligands), and Q_{015} (distortions like plane corrugation) behave similarly. They are approximately equal by magnitude, but they have different signs.

AUTHOR INFORMATION

Corresponding Author

*E-mail: lamonova@fti.dn.ua. Phone: +3 (062) 311 53 48. Fax: +3 (062) 342 90 18.

ACKNOWLEDGMENT

This work was supported in part by FRSF of Ukraine Grant No. F29.1/014, a Russian-Ukrainian Grant No. 9-2010, and grant No. 91 of the project No. 126, by RFBR Grants 09-02-00171 and 10-02-00251, and by the Department of Physics of the Russian Academy of Sciences project 3.1.

REFERENCES

(1) Podlesnyak, A.; Conder, K.; Pomjakushina, E.; Mirmelstein, A. Layered Cobalt Perovskites: Current Topics and Future Promises. In *Frontal semiconductor research*; Nova Science Publishers, Inc.: New York, 2006.

(2) Ivanova, N.; Ovchinnikov, S.; Korshunov, M.; Eremin, I.; Kazak, N. *Phys.Usp.* **2009**, *52*, 789–810.

(3) Korotin, M. A.; Ezhov, S. Yu.; Solovyev, I. V.; Anisimov, V. I.; Khomskii, D. I.; Sawatzky, G. A. *Phys. Rev. B* **1996**, *54*, 5309–5316.

(4) Fita, I.; Szymczak, R.; Puzniak, R.; Wisniewski, A.; Troyanchuk, I. O.; Karpinsky, D. V.; Markovich, V.; Szymczak, H. *Phys. Rev. B* **2011**, *83*, 064414-8.

(5) Nakajima, T.; Ichihara, M.; Ueda, Yu. *J. Phys. Soc. Jpn.* **2005**, *74*, 1572–1577.

(6) Kundu, A. K.; Rautama, E.-L.; Boullay, Ph.; Caignaert, V.; Pralong, V.; Raveau, B. *Phys. Rev. B* **2007**, *76*, 184432-4.

(7) Gatteschi, D.; Bogani, L.; Cornia, A.; Mannini, M.; Sorace, L.; Sessoli, R. *Solid State Sci.* **2008**, *10*, 1701–1709.

(8) Cambi, L.; Szego, L. *Ber. Dtsch. Chem. Ges.* **1931**, *64*, 259–264.

(9) Miller, J. S.; Epstein, A. J.; Reiff, W. M. *Science* **1988**, *240*, 40–47.

(10) Itoh, K., Kinoshita, M., Eds. *Molecular Magnetism: New Magnetic Materials; Kodansha and Gordon and Breach*; Science Publishers: Tokyo and Amsterdam, 2000.

(11) Cavallini, M.; Facchini, M.; Albonetti, C.; Biscarini, F. *Phys. Chem. Chem. Phys.* **2008**, *10*, 784–793.

(12) Ovchinnikov, S. G.; Orlov, Yu. S. *ZhETF* **2007**, *104*, 436–444.

(13) Van Vleck, J. H. *Phys. Rev.* **1932**, *41*, 208–215.

(14) Sugano, S.; Tanabe, Y.; Kamimura, H. *Multiplets of Transition-Metal Ions in Crystals*; Academic Press: New York, 1970.

(15) Zhitlukhina, E. S.; Lamonova, K. V.; Orel, S. M.; Pashkevich, Yu. G. *Low Temp. Phys.* **2005**, *31*, 963–970.

(16) Zhitlukhina, E. S.; Lamonova, K. V.; Orel, S. M.; Lemmens, P.; Pashkevich, Yu. G. *J. Phys.: Condens. Matter* **2007**, *119*, 156216-15 pp.

(17) Babkin, R. Yu.; Lamonova, K. V.; Orel, S. M.; Pashkevich, Yu. G. *Opt. Spectrosc.* **2009**, *107*, 9–15.

(18) Slater, J. C. *Phys. Rev.* **1930**, *36*, 57–64.

(19) Bersuker, I. B. *Electronic Structure and Properties of Transition Metal Compounds: Introduction to the Theory*; Wiley-Interscience: New York, 1996.

(20) Shannon, R. D. *Acta Crystallogr.* **1972**, *A32*, 751–767.

(21) Vonsovskii, S. V.; Grum-Grzhimailo, V. S.; Cherepanov, V. I.; Men', A. N.; Sviridov, D. T.; Smirnov, Yu F.; Nikiforov, A. E. *Crystal Field Theory and Optical Spectra of Ions with an Incomplete d Level*; Nauka: Moscow, 1969 (in Russian).

(22) Sommerfeld, A.; Wentzel, G. Z. *Phys.* **1921**, *7*, 86–92.

(23) Pauling, L. *Proc. R. Soc.* **1927**, *A 114*, 181-211.

(24) Angus, W. *Proc. R. Soc. A* **1932**, *136*, 569–578.

(25) Kohlrausch, K. *Acta Phys. Austriaca* **1950**, *3*, 458–478.

(26) Urusov, V. S. *J. Struct. Chem.* **1962**, *3*, 437–440 (in Russian).

(27) Lamonova, K.; et al. *J. Phys.: Condens. Matter* **2009**, *21*, 045603-9.

(28) Shapovalov, V. A; et al. *J. Phys.: Condens. Matter* **2010**, *22*, 245504-7.

(29) Asai, K.; Yoneda, A.; Yokokura, O.; Tranquada, J. M.; Shirane, G; Kohn, K. *J. Phys. Soc. Jpn.* **1998**, *67*, 290–296.

(30) Radaelli, P, G.; Cheong, S.-W. *Phys. Rev. B* **2002**, *66*, 094408-9.

(31) Luetkens, H.; Stingaciu, M.; Pashkevich, Yu. G.; Conder, K.; Pomjakushina, E.; Gusev, A. A.; Lamonova, K. V.; Lemmens, P.; Klauss, H.-H. *Phys. Rev. Lett.* **2008**, *101*, 017601-4.

(32) Khomskii, D. I.; Löw, U. *Phys. Rev. B* **2004**, *69*, 184401-4.

(33) Akahoshi, D.; Ueda, Yu. *J. Phys. Soc. Jpn.* **1999**, *68*, 736–739.

(34) Frontera, C.; Garcia-Munoz, J. L.; Llobet, A.; Aranda, M. A. G. *Phys. Rev. B* **2002**, *65*, 180405–180408.

(35) Khalyavin, D. D.; et al. *Phys. Rev. B* **2003**, *67*, 214421-5.

(36) Khalyavin, D. D.; Argyriou, D. N.; Amann, U.; Yaremchenko, A. A.; Kharton, V. V. *Phys. Rev. B* **2007**, *75*, 134407-14.